

Tools for reactor evaluation in bioprocesses

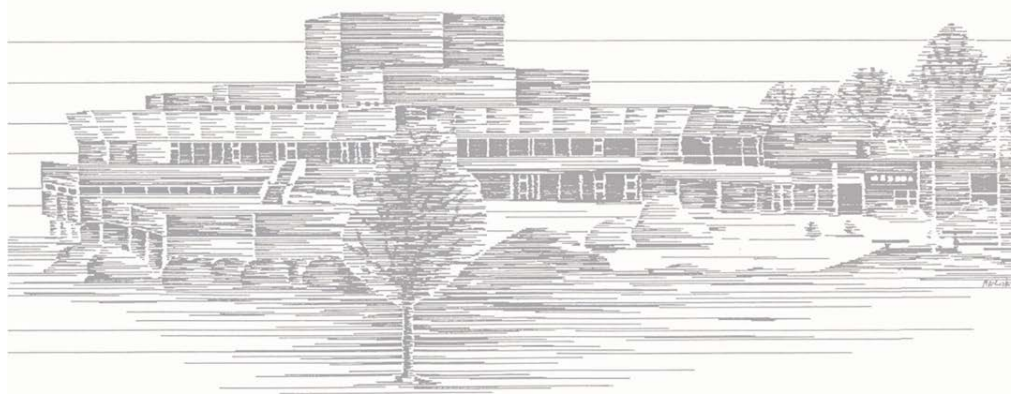
Petri Tervasmäki, Dmitry Gradov, Marko Latva-Kokko, Tuomas Koironen, Juha Tanskanen

Manuscript published as chapter of:

Book of Proceedings of STEP_sCON 2018

STEP_sCON 2018 – International Scientific Conference
on Sustainability and Innovation

7 December 2018, Leverkusen, Germany



Technology
Arts Sciences
TH Köln

Tools for reactor evaluation in bioprocesses

Petri Tervasmäki^{1*}, Dmitry Gradov², Marko Latva-Kokko³, Tuomas Koiranen², Juha Tanskanen¹

¹ Chemical Process Engineering, University of Oulu, P.O. Box 4000, FI-90014 Oulu, Finland,

² School of Engineering Science, Lappeenranta University of Technology, P.O. Box 20, FI-53851 Lappeenranta, Finland

³ Outotec (Finland) Oy, Outotec Research Center, P.O. Box 69, FI-23101 Pori, Finland

*Corresponding author, Email: petri.tervasmaki@oulu.fi

Abstract

Aerobic microbial cultivations are industrially important group of processes and pose challenges for the reactor design. In particular, estimation of industrial scale conditions is difficult from laboratory and pilot scale data. Due to complex interaction of gas/liquid phase hydrodynamics, mass transfer parameters and microbial metabolism, both improvement of modelling tools and reactor design are desired. We present an approach to estimate growth conditions in industrial scale reactor by combining black-box metabolic models with CFD-model.

The reactor type used here is Outotec OKTOP9000[®], which is used in the industrial hydrometallurgical processes at 900 m³ scale. It is adopted to a laboratory setting and compared to stirred tank reactor (STR) in gas dispersion, mass transfer and yeast cultivation experiments. In addition, a kinetic model for the yeast growth is developed based on literature sources and validated by the laboratory scale batch cultivations. This kinetic model is used along with CFD-model that is developed to describe the flow and mass transfer conditions in the industrial scale reactor.

The laboratory scale experiments show the feasibility of OKTOP9000[®] reactor when compared to STR, particularly with improved gas handling capacity. The modelling approach shows qualitatively similar behavior in the large scale simulations when compared to laboratory scale cultivations.

1. Introduction

Aerobic microbial cultivations pose challenges for the design of industrial reactors. One limitation for the process performance is often the interfacial mass transfer rate of oxygen from gas to liquid phase. Furthermore, due to high oxygen demand of the process, air is introduced into the reactors with relatively high flow rate thus affecting the hydrodynamics of the reactor. There are complex interactions between the hydrodynamics, mass transfer parameters and microbial growth. Since the scale of the process affects in a different way for

each phenomena, it is difficult to generalize experimental results obtained in the laboratory scale and use them as a basis for industrial scale designs. [1], [2] Simple scale-up rules are often used to estimate the conditions in the large scale based on the results obtained in the laboratory. The most common scale-independent parameters to describe reactor operation include volumetric power input of agitation (P/V in W/m^3) and superficial gas velocity (v_s in m/s), and dimensionless groups such as Froude number and gas flow number. The common measured/estimated parameters are volumetric mass transfer coefficient k_La and gas volume fraction.

However, even the scale-independent and dimensionless correlations include experimental parameters that are only valid for a narrow range of scales. Thus, the correlations are generally not reliable from 100 liter to 100 m^3 reactor, for example [3]. Furthermore, although superficial gas velocity is a feasible scale-independent parameter to describe the hydrodynamic regime of gas flow, constant v_s results in decreasing volumetric gas input measured in volume gas per volume liquid per minute (VVM). The latter would be a desired approach for scaling up the gas flow in the stoichiometric point of view but would result in too high gas flow when the hydrodynamics are also considered. In fact, in scaling up industrial processes, the value of VVM is usually decreased while v_s is increased so that stirred tank reactors are operated in the loading regime with insufficient gas recirculation at the lowest impeller [4].

Here we present results from studies of new reactor type for industrial scale aerobic microbial processes with modelling approach to estimate the growth conditions in the large scale. The original research has been published in [5]–[7], and the main results are presented here. The reactor used in the studies is Outotec OKTOP9000[®] reactor with draft tube and a single agitator placed below the draft tube. The impeller creates downward flow inside the draft tube while dispersing inflowing gas, introduced under the impeller, radially. It has been developed for direct leaching of zinc concentrate and designed to have good gas dispersion and mass transfer capacity and bulk liquid circulation at low power input. Laboratory scale experiments for gas dispersion and mass transfer rate are carried out with stirred tank reactor (STR) as a reference. A growth model for oxygen sensitive yeast is developed in the laboratory scale and combined with CFD-model to simulate growth conditions in the industrial scale. The industrial scale reactor and adaptation to CFD-model are presented in Figure 1.



Figure 1. Industrial scale OKTOP®9000 reactor (left) and CAD geometry for large-scale reactor and impeller (right). Adapted with permission from Outotec Oyj

2. Materials and Methods

2.1 Reactor types and mixing / mass transfer experiments

Experiments were carried out in laboratory scale Biostat C (Sartorius, Germany) reactor with a total volume of 15 liters and a diameter of 190 mm. The OKTOP9000® reactor was constructed in the same vessel from stainless steel parts except the impeller, which was 3D-printed from alumina reinforced plastic. Regular stirred tank reactor (STR) with three Rushton turbines was used as a reference, and the reactor geometries are shown in Figure 2. The electrical impedance tomography (EIT) measurements were carried out in plastic (PMMA) vessels with similar geometry as the Biostat C. The 32 electrodes in the EIT-vessel were distributed in four layers (at 4.5, 12.9, 25.5 and 33.9 cm heights) with eight electrodes each. Current injection was made by a modified opposite injection pattern with 0.7 A amplitude at 10 kHz frequency. The EIT-measurements give directly the estimated three-dimensional conductivity distribution, from which the distribution of local gas volume fraction can be estimated by Maxwell model with an assumption that the conductivity of the dispersed phase (air) is zero. Overall gas-liquid mass transfer coefficient ($k_L a$) was estimated

by gas in / gas out experiments using air and nitrogen, respectively. The value for $k_L a$ was estimated from the saturation phase using probe response time of 15 s, plug flow model for gas, and ideally mixed assumption for the liquid phase. More detailed procedures are described in [5].

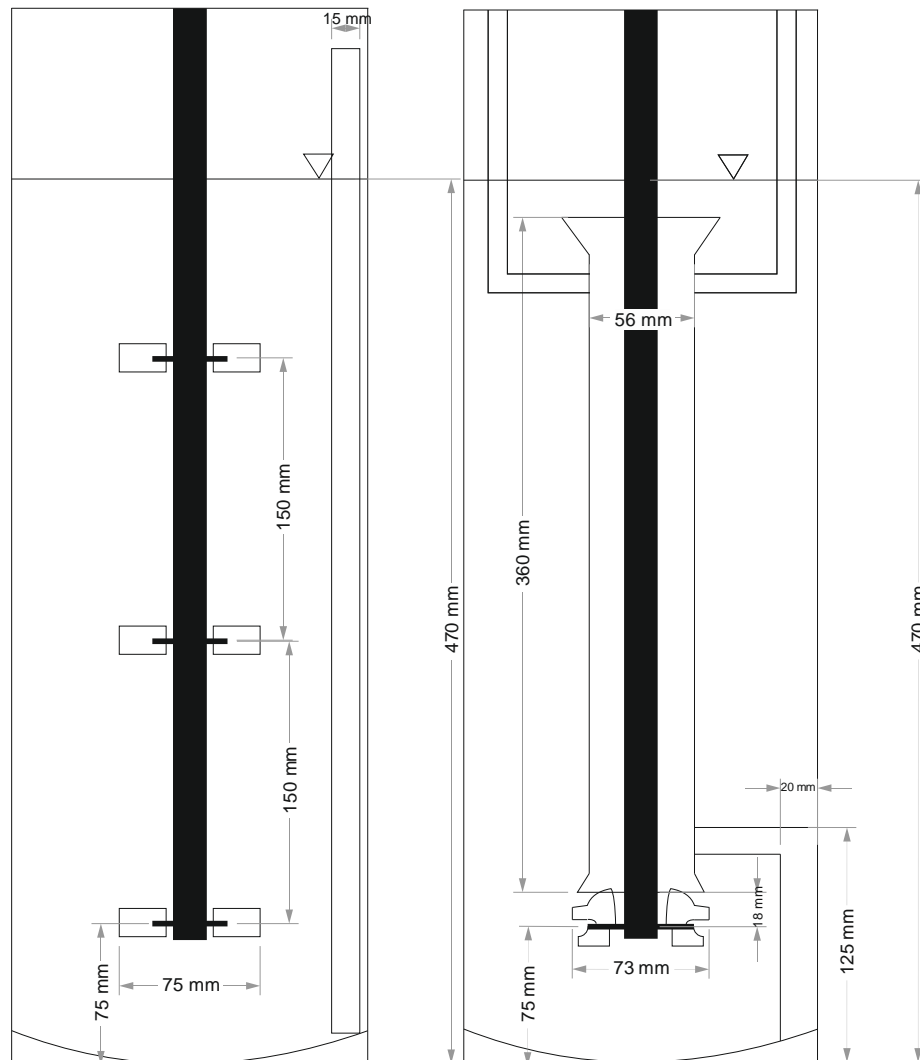


Figure 2. Stirred tank and OKTOP9000® reactor geometries in laboratory scale. Reprinted with permission from Elsevier [5]

2.2 Yeast cultivations

Yeast cultivations were carried out with *Pichia pastoris* X33 yeast strain and basal salt medium (BSM) with PTM₁-trace salt supplement in the reactors described in the previous chapter. Glucose concentration was 80 g/l. Aqueous ammonium hydroxide (25 %) was used to maintain pH between 5.0 – 5.5, pH was measured with EasyFerm Plus pH-electrode (Hamilton, Switzerland) and dissolved oxygen with Oxyferm (at 10 cm from vessel bottom) and Visiferm (at 10 cm from surface) DO-probes (Hamilton, Switzerland). Gas flow rate was maintained at 18 l/min, which results in superficial gas velocity $v_s = 0.011$ m/s. Agitation rate was 450 rpm (STR) or 650 rpm (OKTOP9000®) which yielded in mixing power of about 500 W/m³ for each reactor.

2.3 Kinetic model

The full description of the model can be found in [6], and a short summary is presented here. The three metabolic routes are schematically presented in Figure 3 and in equations (1)-(3). The aim is to describe respirative metabolism on glucose (blue, equation (1)), fermentative metabolism on glucose if oxygen supply is limited/unavailable (red, equation (2)), and respirative metabolism on ethanol (purple, equation (3)). The growth kinetics are described with Monod-type equations for the substrate uptake rate (glucose equations (1)-(2) or ethanol equation (3)) with additional terms for oxygen.

$$q_g^{\text{ox}} = \frac{\mu_{\text{max}}^{\text{ox}}}{Y_{\text{xg}}^{\text{ox}}} \frac{c_g}{c_g + K_g} \frac{c_o}{c_o + K_o} \quad (1)$$

$$q_g^{\text{ferm}} = \frac{\mu_{\text{max}}^{\text{ferm}}}{Y_{\text{xg}}^{\text{ferm}}} \frac{c_g}{c_g + K_g} \left(1 - \frac{c_o}{c_o + K_o}\right) \quad (2)$$

$$q_e^{\text{ox}} = \frac{\mu_{\text{max}}^e}{Y_{\text{xe}}^{\text{ox}}} \frac{c_e}{c_e + K_e} \frac{K_i}{c_g + K_i} \frac{c_o}{c_o + K_o} \quad (3)$$

Where q_i is specific rate of component i ($\text{g}_i \text{g}_x^{-1} \text{h}^{-1}$) and x, g, e and o denote cells, glucose, ethanol and oxygen, respectively. K_i is the saturation concentration of Monod-type kinetics, c_i is the concentration of component i , and μ_{max} and Y are parameters for maximum growth rate and yield coefficient.

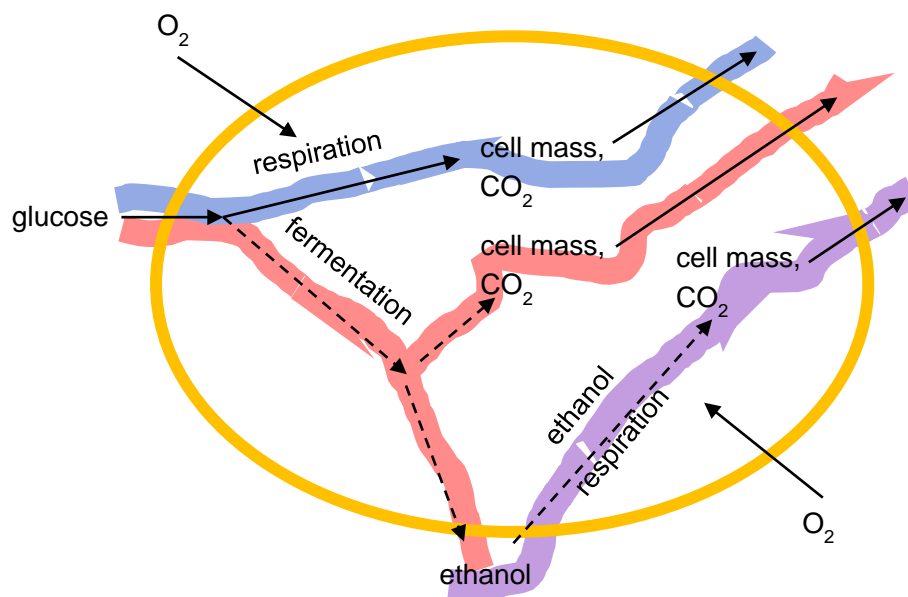


Figure 3. A schematic presentation of the main metabolic routes included in the model

2.3 CFD model

CFD-model of industrial scale OKTOP9000[®] reactor ($T = 7.6$ m, $V = 800$ m³) was developed in ANSYS Fluent 18 with user defined functions to accommodate the yeast growth model. Eulerian-Eulerian multiphase approach was used to simulate gas-liquid flow, and Reynolds-averaged Naviers Stoke's (RANS) with realizable k - ϵ model was used to model turbulence. More information on the assumptions regarding phase interaction, boundary conditions, the estimation of mass transfer conditions based on the converged CFD-model, and inclusion of the yeast growth kinetics can be found in the original publication [7]. A schematic presentation of the numerical approach is in Figure 4.

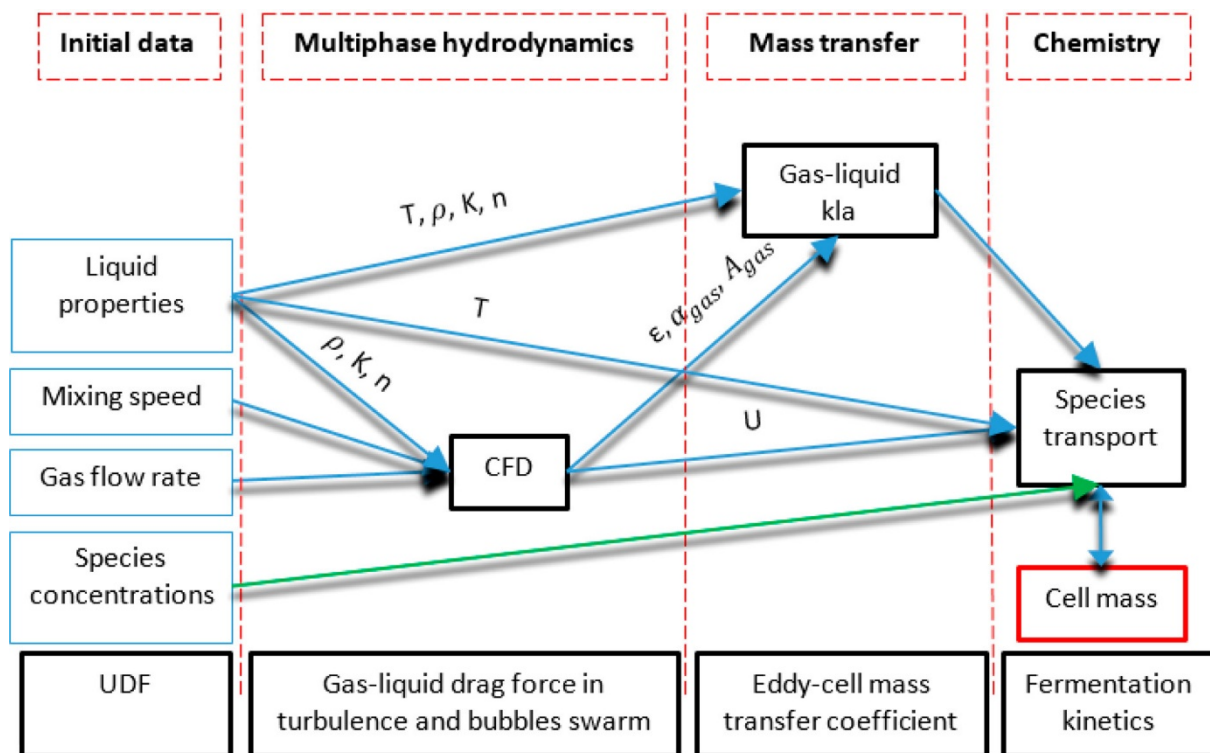


Figure 4. Numerical approach for the combined CFD, mass transfer and yeast growth model simulations. Reprinted from [7] under CC-BY license.

3. Results & Discussion

3.1 Yeast model

The model parameters were estimated based on literature data from chemostat cultivations with varying glucose feed concentration, dilution rate and oxygen content in the inlet gas [8]–[11]. In addition, the reactor setup was different in the experiments and a relative value for $k_L a$ was estimated based on the reported geometry and operational conditions. The simulated values for steady-state concentrations of cell mass, ethanol, and dissolved oxygen (DO) are shown in Figure 5. The effect of oxygen content on the concentrations at constant inlet glucose concentrations and dilution rate is shown in (a) and a parity plot for all

experiments in (b). The calibrated model can fit the literature data quite well although there are some deviation especially for the ethanol concentration. For validation, the model was used to predict the time course of batch cultivation with initial glucose concentration of 40 g/l. The agitation and aeration were maintained constant and, thus, a constant value for $k_L a$ was assumed. The results are shown in Figure 6 for glucose, ethanol and cell mass (a) and dissolved oxygen (b) concentrations.

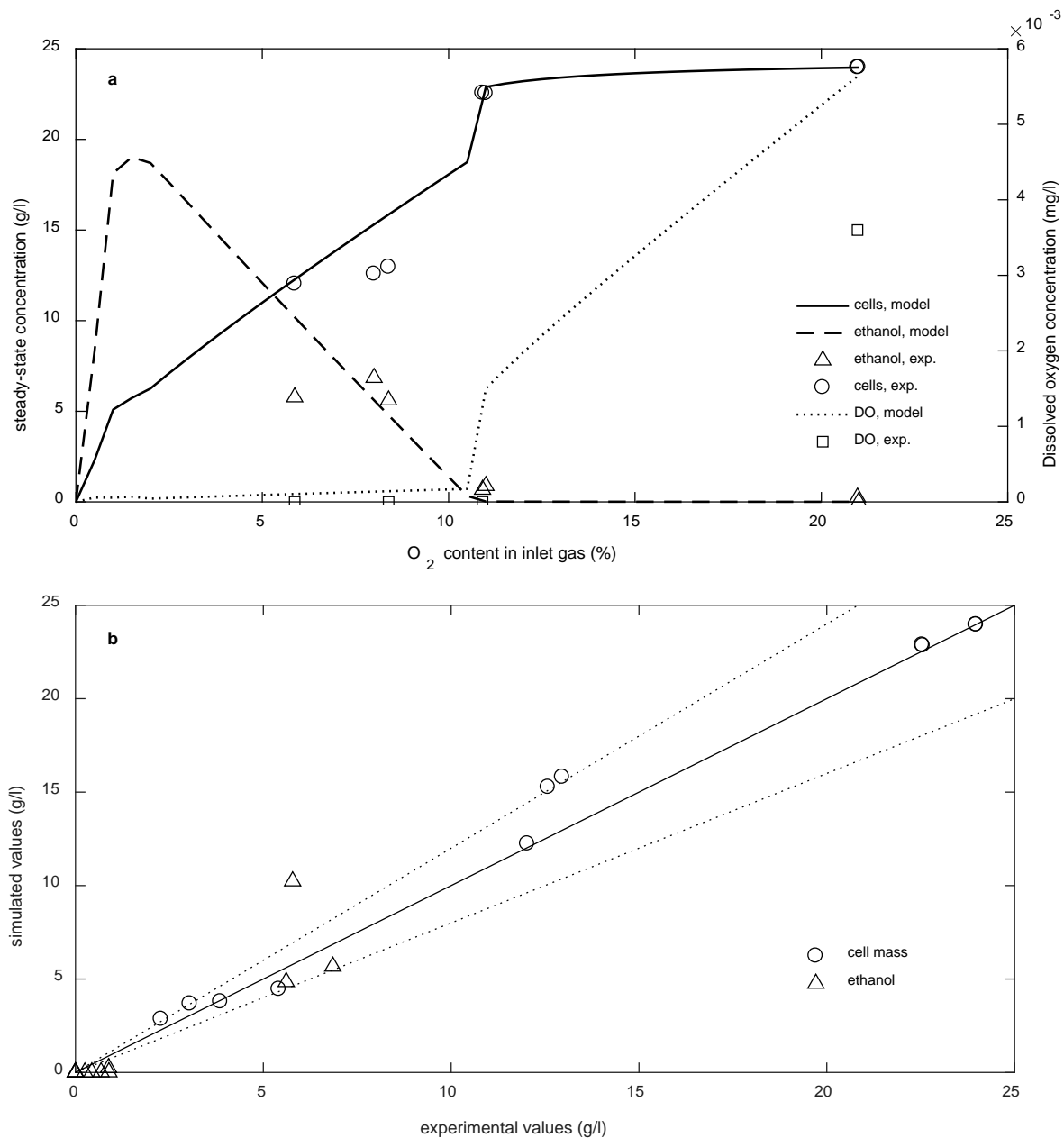


Figure 5. a) Steady-state concentration of cell mass, ethanol and DO (experimental and simulated) gas for $c_{g,in} = 50$ g/l and $D = 0.1$ h⁻¹ as reported in [10], [11]. b) Simulated and experimental values for steady-state concentration of cell mass and ethanol in all chemostat cultivation conditions in the literature, dotted lines show $\pm 20\%$ margin. Reprinted from [6] with permission from Elsevier.

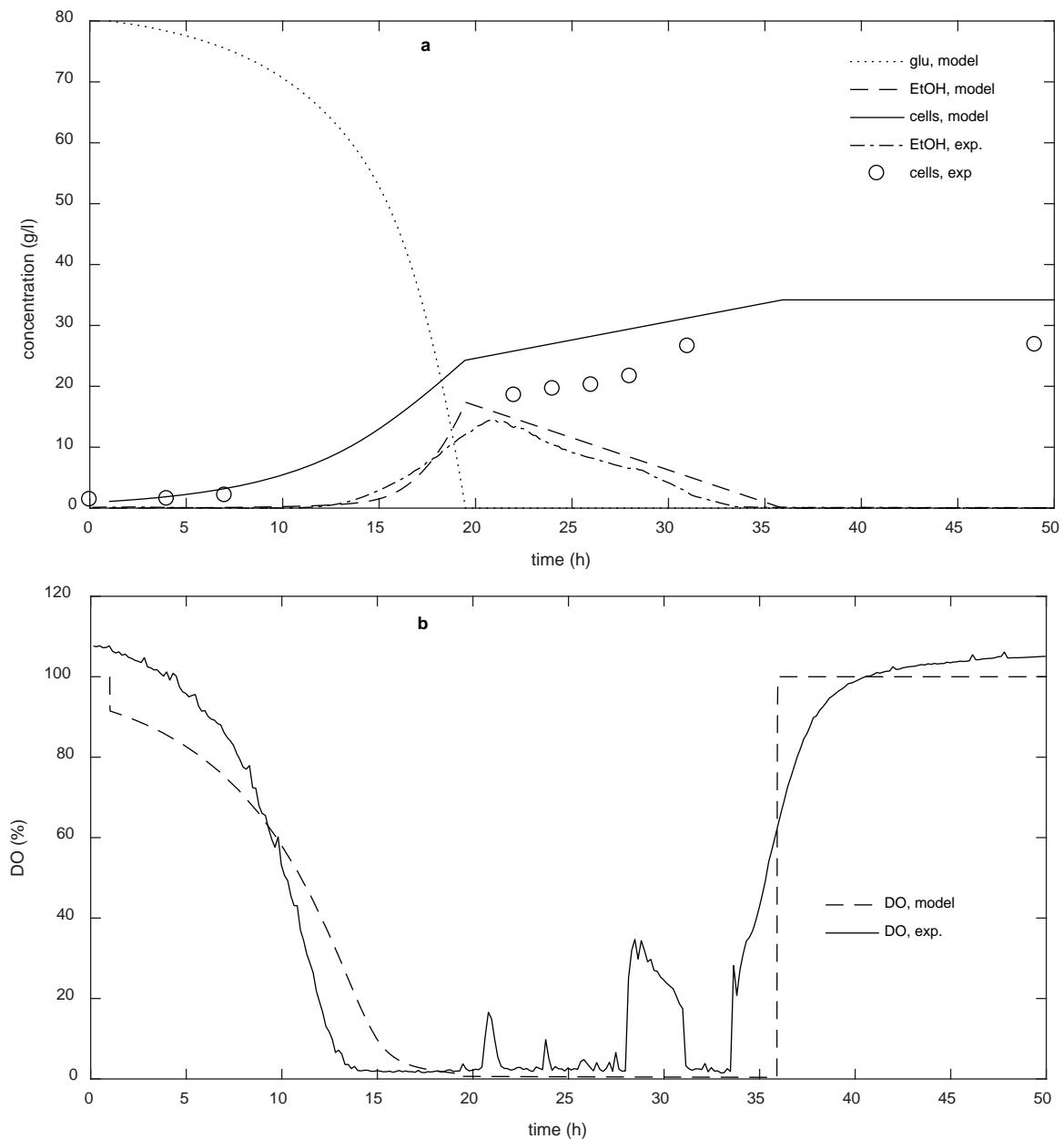


Figure 6. Comparison of model prediction to batch cultivation data in STR, additional lag time of one hour was added to the model prediction. Estimated $k_L a$ for the simulations was 250 h^{-1} a) glucose, ethanol and cell concentration b) dissolved oxygen. Reprinted from [6] with permission from Elsevier.

Three main phases can be distinguished from the batch cultivation. The first phase lasts until about 14 hours, during which glucose is consumed via fully respiratory metabolism. However, due to increase in cell concentration, the dissolved oxygen drops to almost zero, which results in respirofermentative metabolism, during which glucose is utilized to produce both cell mass and ethanol. This phase lasts until 21 hours after which glucose is exhausted, and peak ethanol concentration reaches 14 g/l. After this, until about 34 hours, ethanol is aerobically consumed for cell mass production although with lower growth rate. The model captures well the main phases of the batch cultivation. Only the cell mass is somewhat over

predicted. In addition, the model fails to capture the short peak in dissolved oxygen at 21 when the yeast switches the carbon source from glucose to ethanol. This is expected, as the model does not include detailed metabolism and enzyme kinetics inside the cell. The short increase in DO between 28 and 31 hours is due to temporary increase in the agitation during the experiment, and the model prediction was calculated with constant k_La . Model sensitivity analysis is presented in [6], and a more detailed global parameter analysis and model refinement is being planned for future work.

3.2 Mixing and mass transfer experiments in lab scale

The performance of OKTOP9000® reactor was tested in the laboratory scale and compared to traditional STR with three Rushton turbines. The results for gas distribution with constant agitation rate and varying gas feed rates are presented in Figure 7 for both reactor types. The results were averaged over the whole measurement volume and are presented as two-dimensional plane. One can directly see that the gas hold-up is more uniform in the STR whereas the gas is more concentrated on the bottom part in the OKTOP9000® reactor. However, due to more efficient overall circulation and less compartmentalization, the uneven distribution of gas is not necessarily a downside. Complete dispersion is achieved only with the lowest gas flow rate for both reactors. This was confirmed visually, and can be interpreted from the EIT-measurements as it is the only measurement at which the highest gas hold-ups are detected below the impeller plane and extending near the reactor wall.

With increasing air flow, the bubbles are not fully recirculated in the lower parts of the reactors. Increasing the air flow in the OKTOP9000® reactor shifts the highest gas volume fractions more in the annulus part around the draft tube. For the STR, the effect is more drastic as the lowest impeller is loaded with no significant radial distribution of the gas. For the highest gas flow, the gas is fully distributed only at the highest impeller which can be seen as the gas hold-up is concentrated in the upper part. It should be noted that the spatial resolution of the EIT-measurements is not high enough to catch very high volume fractions at the center of the reactor or around the impeller blades. The measurements of k_La are presented in Figure 8 for the whole measurement range, and the values for $P/V = 500 \text{ W/m}^3$ are in the range of $0.04 - 0.07 \text{ s}^{-1}$.

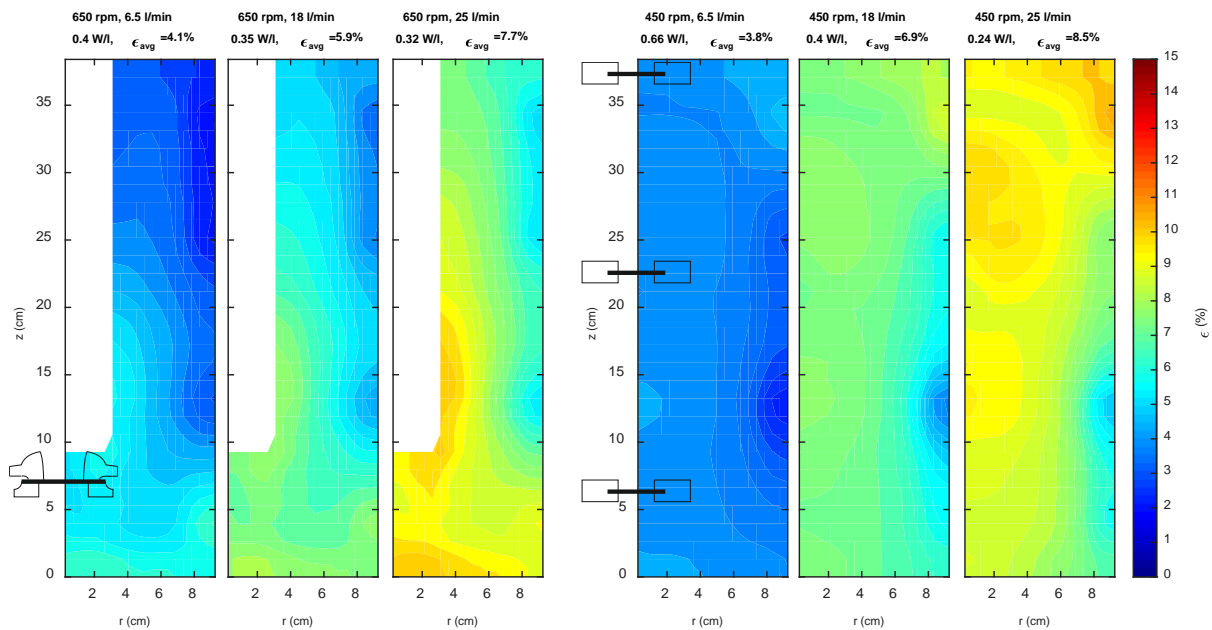


Figure 7. EIT results with constant agitation rate and varying gas flow rate for OKTOP9000® (left) and STR (right). The gas flow rates 6.5, 18 and 25 l/min correspond to v_g of 0.004, 0.011 and 0.015 m/s.

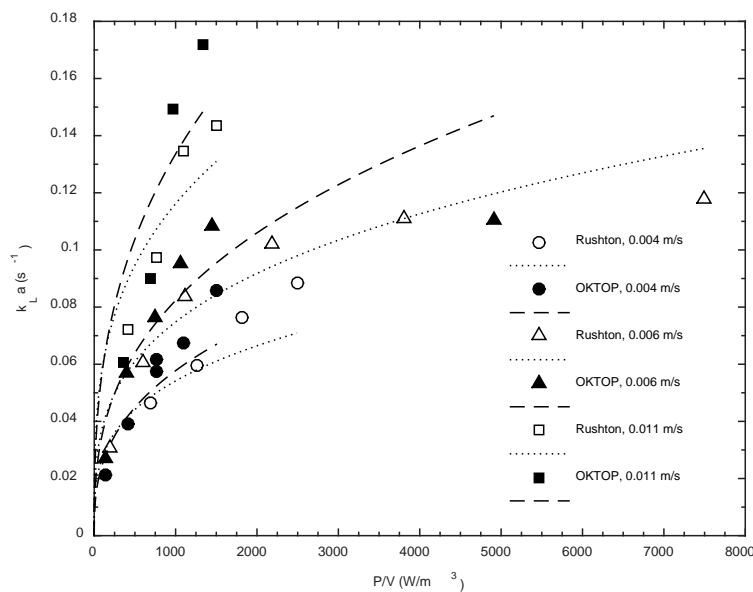


Figure 8. Estimated $k_L a$ -values from gas in / gas out experiments. Reprinted from [5] with permission from Elsevier.

3.3 OKTOP CFD model & simulations

The CFD-model was simulated with gas flow rates of 0, 2000, 4000 and 6000 m³/h, corresponding to superficial gas velocities of 0, 0.012, 0.024 and 0.037 m/s. The stirrer speed was 60 rpm, corresponding to volumetric power input of about 500 W/m³. The corresponding liquid flow velocities are presented in Figure 9. The radial flow from the impeller is pushed upward by the gas flow, and this effect is more significant with increasing gas flow. It can also be seen that the downward flow velocity inside the draft tube decreases

with increasing gas flow. Near the solution surface, the flow velocities are more affected by the gas escaping the liquid.

For the estimation of mass transfer and cultivation conditions, additional values were estimated from the CFD-simulation. Sauter mean diameter (d_{32}) of the bubbles and local $k_L a$ are presented in Figure 10. The bubble size is at minimum in the most turbulent regions of the radial flow near the impeller and higher values are found under the impeller and in the central area close to the liquid surface. It can also be noted that the increase in gas flow increases the bubble size below the impeller, which results from the lower liquid velocities (Figure 9). Similar trends can be seen for the specific mass transfer coefficient in Figure 10. Highest values for $k_L a$ are near the impeller. The increase in gas flow rate increases the values especially in the upper part of the annulus and in the draft tube of the reactor.

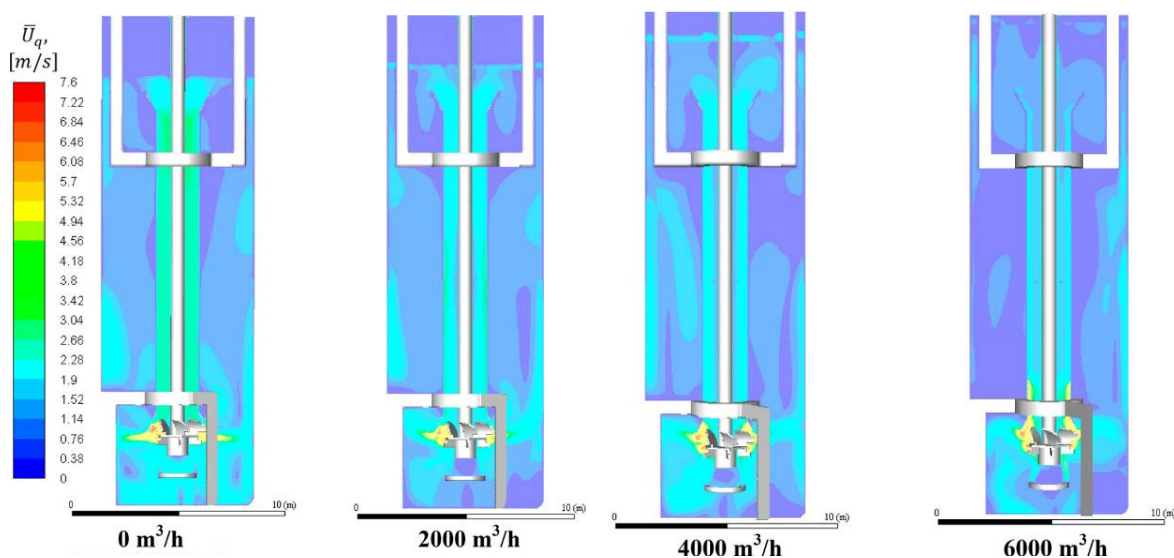


Figure 9. Liquid flow velocity in the converged CFD-simulations with varying gas flow rate. Reprinted from [7] under CC-BY license.

Finally, the growth model of *Pichia pastoris* and the CFD-models were combined to simulate a batch cultivation in the industrial scale reactor with the approach shown in the Figure 4. The initial conditions were similar as for the laboratory cultivations with initial glucose and cell concentrations of 80 g/l and 2 g/l, respectively. The results are presented in Figure 11 for glucose, ethanol and cell concentrations. The batch simulations were carried out with the gas flow rates reported previously (2000, 4000 and 6000 m₃/h), and the experimental values from laboratory cultivations are included in the figure. The simulations in the CFD-model follow qualitatively the results from the laboratory experiments. Similar phases of batch process can be distinguished. Ethanol is produced in the beginning of the process due to oxygen limitation, and ethanol is consumed in the later phase. Moreover, the maximum ethanol concentration depends on the gas flow rate and less ethanol is produced in the simulations with increasing gas flow, resulting in better oxygen transfer conditions.

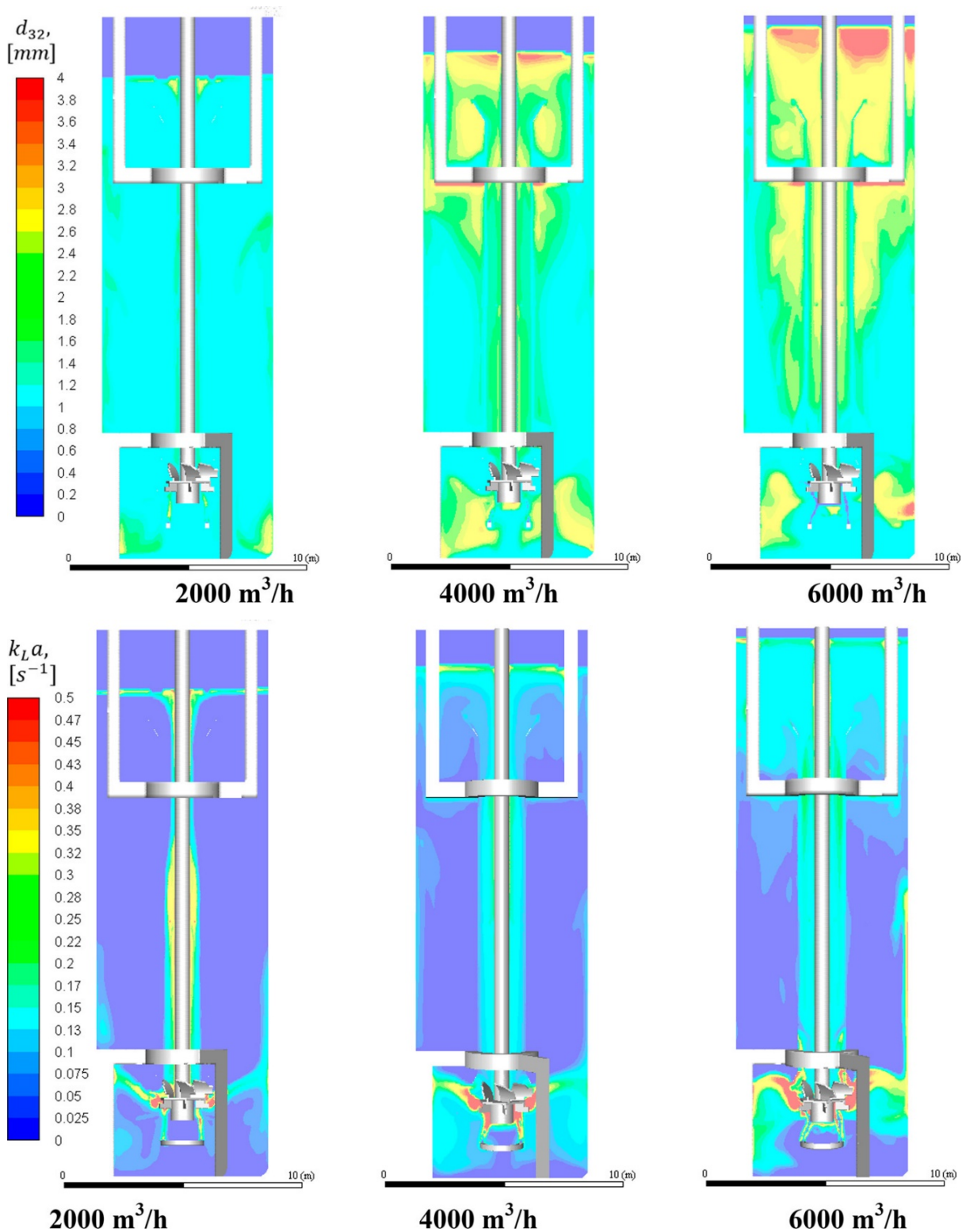


Figure 10. Mean sauter diameter (d_{32} , upper row) and $k_L a$ (lower row) estimated from the CFD-simulations with varying gas flow rate. Reprinted from [7] under CC-BY licence.

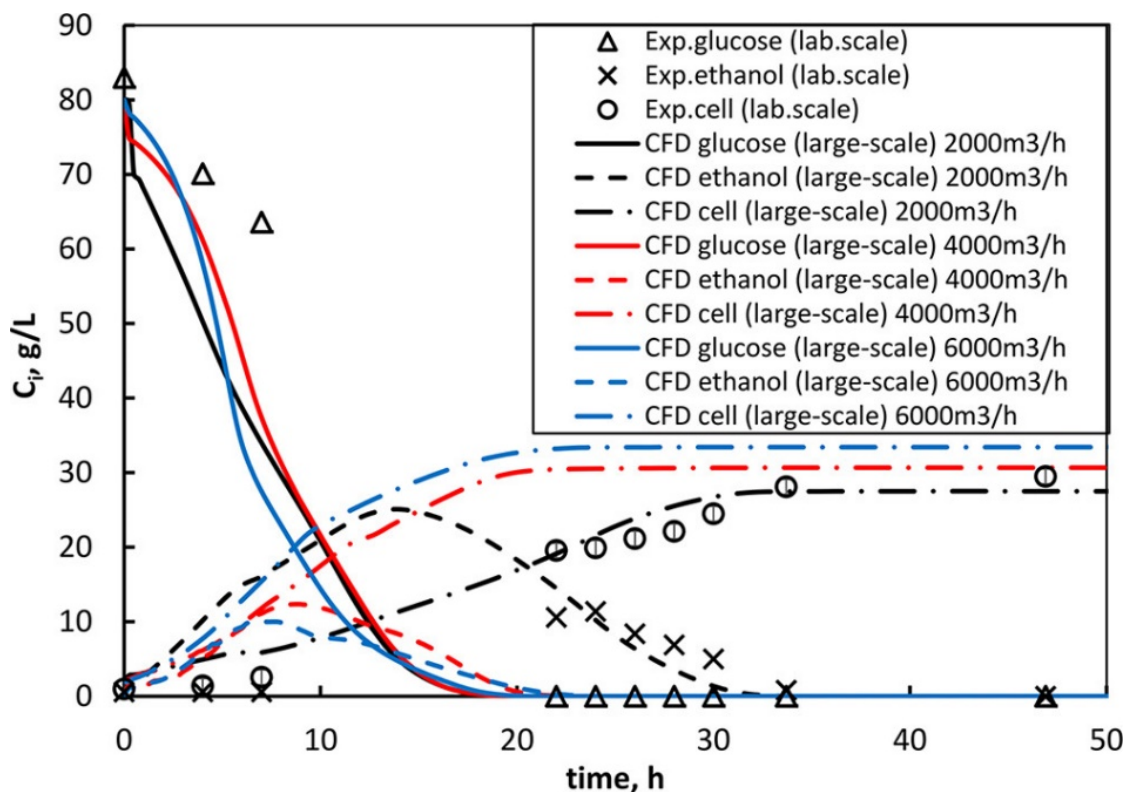


Figure 11. Time-course data from the simulations of batch cultivation with varying gas flow rate. Reprinted from [7] under CC-BY licence.

Conclusions

In the studies presented above, we have developed and validated a growth model for *Pichia pastoris* in the laboratory scale. Furthermore, the reactor concept of OKTOP9000® draft tube reactor was adopted for laboratory scale in which it performed well in mixing and mass transfer experiments when compared to regular STR. CFD-model was implemented to simulate flow conditions in the industrial scale OKTOP9000® reactor with estimation of relevant mass transfer parameters. By adopting the growth model into the CFD-model, we simulated time course data of batch yeast cultivation. These results showed qualitative agreement with the laboratory scale cultivation data. The validation of the CFD-model and the refinement of yeast growth model are left for future work.

Acknowledgements

The authors are grateful to the Finnish Funding Agency TEKES and, in particular, to Outotec Finland Oy and Neste Engineering Solutions Oy collaborating under FERMATRA project (908/31/2016 and 958/31/2016), for active supervision and financial support.

References

- [1] F. Garcia-Ochoa and E. Gomez, 'Bioreactor scale-up and oxygen transfer rate in microbial processes: An overview', *Biotechnology Advances*, vol. 27, no. 2, pp. 153–176, 2009.
- [2] F. Garcia-Ochoa, E. Gomez, V. E. Santos, and J. C. Merchuk, 'Oxygen uptake rate in microbial processes: An overview', *Biochemical engineering journal*, vol. 49, no. 3, pp. 289–307, 15 2010.
- [3] E. K. Nauha, O. Visuri, R. Vermasvuori, and V. Alopaeus, 'A new simple approach for the scale-up of aerated stirred tanks', *Chemical Engineering Research and Design*, vol. 95, pp. 150–161, 2015.
- [4] E. K. Nauha, Z. Kálal, J. M. Ali, and V. Alopaeus, 'Compartmental modeling of large stirred tank bioreactors with high gas volume fractions', *Chemical Engineering Journal*, vol. 334, pp. 2319–2334, Feb. 2018.
- [5] P. Tervasmäki, M. Latva-Kokko, S. Taskila, and J. Tanskanen, 'Mass transfer, gas hold-up and cell cultivation studies in a bottom agitated draft tube reactor and multiple impeller Rushton turbine configuration', *Chemical Engineering Science*, vol. 155, pp. 83–98, Nov. 2016.
- [6] P. Tervasmäki, M. Latva-Kokko, S. Taskila, and J. Tanskanen, 'Effect of oxygen transfer on yeast growth — Growth kinetic and reactor model to estimate scale-up effects in bioreactors', *Food and Bioproducts Processing*, vol. 111, pp. 129–140, Sep. 2018.
- [7] D. V. Gradov *et al.*, 'Numerical Simulation of Biomass Growth in OKTOP®9000 Reactor at Industrial Scale', *Ind. Eng. Chem. Res.*, vol. 57, no. 40, pp. 13300–13311, Oct. 2018.
- [8] M. Carnicer *et al.*, 'Quantitative metabolomics analysis of amino acid metabolism in recombinant *Pichia pastoris* under different oxygen availability conditions', *Microbial Cell Factories*, vol. 11, p. 83, Jun. 2012.
- [9] A. Solà, H. Maaheimo, K. Ylönen, P. Ferrer, and T. Szyperski, 'Amino acid biosynthesis and metabolic flux profiling of *Pichia pastoris*', *European Journal of Biochemistry*, vol. 271, no. 12, pp. 2462–2470, Jun. 2004.
- [10] K. Baumann *et al.*, 'A multi-level study of recombinant *Pichia pastoris* in different oxygen conditions', *BMC Syst Biol*, vol. 4, p. 141, Oct. 2010.
- [11] K. Baumann, M. Maurer, M. Dragosits, O. Cos, P. Ferrer, and D. Mattanovich, 'Hypoxic fed-batch cultivation of *Pichia pastoris* increases specific and volumetric productivity of recombinant proteins', *Biotechnol. Bioeng.*, vol. 100, no. 1, pp. 177–183, May 2008.